Mixed-Metal Aggregates

DOI: 10.1002/anie.201308090

Clamshell Opening in the Mixed-Metal Supramolecular Aggregates Formed by Fourfold Reduced Corannulene for Maximizing Intercalated Metal Content**

*Alexander S. Filatov, Alexander V. Zabula, Sarah N. Spisak, Andrey Yu. Rogachev, and Marina A. Petrukhina**

Dedicated to Professor Roald Hoffmann on the occasion of his 75th birthday

Abstract: *The first members of a new class of supramolecular organometallic compounds with mixed-alkali-metal cluster cores, LiK_5 and Li_3K_3, sandwiched between two four-fold reduced corannulene decks are prepared and fully characterized. The triple-decker supramolecular anions, $[(C_{20}H_{10}^{4-})(LiK_5)^{6+}(C_{20}H_{10}^{4-})]^{2-}$ and $[(C_{20}H_{10}^{4-})(Li_3K_3)^{6+}(C_{20}H_{10}^{4-})]^{2-}$, illustrate a record ability of bowl-shaped and highly charged corannulene to provide all its sites, five benzene rings fused to a central five-membered ring, for binding of six alkali-metal ions. The previously unseen engagement of the hub-site of $C_{20}H_{10}^{4-}$ in lithium binding is accompanied by unprecedented shifts up to −24 ppm in ^{7}Li NMR spectra. The discussion of product formation mechanism, augmented by calculations, is provided.*

The multi-electron reduction processes of curved carbon-rich compounds attract special attention owing to interesting thermoelectric and superconductive properties of products[1] and their advanced performance in lithium-ion batteries.[2] Geodesic polyaromatic compounds are known to readily acquire multiple electrons upon reduction with alkali metals. C_{60}-fullerene can potentially accept up to six extra electrons owing to its triply degenerate and low-lying LUMOs.[3] While all six reduction steps were observed in solution by cyclic voltammetry,[4] so far only mono- through tetraanions[5] of C_{60} have been crystallographically characterized. The smallest non-planar fragment of the C_{60}-fullerene, corannulene ($C_{20}H_{10}$; Scheme 1), has a doubly degenerate LUMO and can thus accept up to four electrons. In reduction reactions with a variety of alkali metals, corannulene readily acquires up to two electrons.[6] A trianionic state has been detected electrochemically[7] but still awaits for its adequate characterization by other methods. The highest reduction state of corannulene, $C_{20}H_{10}^{4-}$, has been clearly identified in the reactions with Li metal,[8] where the stabilization of tetraanion is achieved through the formation of supramolecular aggregates with small lithium ions.[9] While the supramolecular aggregation of corannulene anions has been extensively investigated by the groups of Scott and Rabinovitz using solution NMR spectroscopy,[6a,7–9,10] structural identification of the resulting products in the solid state was lagging behind until 2011, when we have accomplished the first crystallographic characterization of the aggregate formed by the highly reduced corannulene with lithium counterions (Scheme 1).[11] A remarkable supramolecular structure with five lithium ions sandwiched between two four-fold reduced corannulene decks has been revealed.

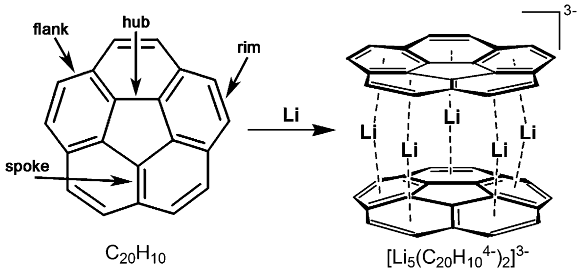

Scheme 1. Preparation of the Li_5 sandwich complex.

Although corannulene was known to be a versatile ligand,[12] for the first time all of its six-membered rings were engaged in metal binding. This unique ability of bowl-shaped polyarene to encapsulate a large number of alkali-metal ions, which can be related to the high charge capacity of the corannulene-based electrodes,[2a] prompted us to further investigate these systems. To maximize the intercalated alkali-metal content, the central hub ring of corannulene, the only unoccupied site in the $[Li_5(C_{20}H_{10}^{4-})_2]^{3-}$ aggregate, has to be engaged in binding. The intercentroid $C_5 \cdots C_5$ distance in the Li_5-sandwich structure[13] is 3.52 Å. For comparison, the

---

[*] Dr. A. S. Filatov, Dr. A. V. Zabula, Dr. S. N. Spisak,
Prof. Dr. M. A. Petrukhina
Department of Chemistry, University at Albany
State University of New York, Albany, NY 12222 (USA)
E-mail: mpetrukhina@albany.edu

Dr. A. V. Zabula
Department of Chemistry, University of Wisconsin-Madison (USA)

Prof. Dr. A. Yu. Rogachev
Department of Biological and Chemical Sciences, Illinois Institute of Technology (USA)

[**] Financial support of this work from the National Science Foundation Award (CHE-1212441) is gratefully acknowledged. The authors thank Dr. A. A. Granovsky and the Firefly team for providing a developing version of the Firefly program package. S.N.S. also thanks the International Centre for Diffraction Data (ICDD) for the 2012 and 2013 Ludo Frevel Crystallography Scholarship.

Supporting information for this article is available on the WWW under http://dx.doi.org/10.1002/anie.201308090.

separation between planes in the charge transfer graphite intercalation compound is 3.72 Å for LiC_6.[14] In lithium cyclopentadienide, $[(\eta^5\text{-Cp})_2Li]^-$, the separation between the five-membered rings is even greater (ca. 4.0 Å).[15] The Li−Cp distances generally range from 3.8 to 4.1 Å in other cyclopentadienide organometallic compounds of lithium.[16] Thus, a Li^+ ion may have some difficulty inserting into the space allocated between the hub sites in the above Li_5 sandwich. To allow this fit and thus to fully utilize all available corannulene binding sites, the two bowls should be moved farther apart. This can be accomplished by using alkali metals having larger ionic radii, such as Na and K, for supramolecular assembly. Inspired by the work of Mulvey group[17] that revealed unique reactivity and synergism of mixed-metal systems in alkali-metal-mediated reactions, we decided to investigate the use of two Group 1 metals in corannulene reduction and intercalation reactions. As a result, the cooperative effect of alkali metals in self-assembly processes was revealed, leading to the discovery of a new class of organometallic supramolecules. Two remarkable mixed-metal products with a maximum amount of alkali-metal ions sandwiched between two non-planar $C_{20}H_{10}$ decks, $[(C_{20}H_{10}{}^{4-})(LiK_5)^{6+}(C_{20}H_{10}{}^{4-})]^{2-}$ and $[(C_{20}H_{10}{}^{4-})(Li_3K_3)^{6+}(C_{20}H_{10}{}^{4-})]^{2-}$, have been isolated and fully characterized in this work. The mechanism of their formation along with other possible Li/K cluster compositions is discussed and augmented by DFT calculations.

The initial reduction of $C_{20}H_{10}$ with mixtures of Li and Na in $[D_8]$THF revealed the formation of the known Li_5 aggregate, identified by a characteristic ^{7}Li NMR singlet at −11.7 ppm.[9,11,18] On the contrary, while the formation of four-fold reduced corannulene was clearly observed in the reaction mixture with Li and K metals, the assignment of the specific products in solution was problematic. Notably, a shorter reaction time was observed for the mixed Li/K system compared to the Li-only reduction, pointing to a synergism of two metals. However, all attempts to crystallize the products from the above reaction mixtures in THF have failed. When THF was replaced by bis(2-methoxyethyl) ether (diglyme), there were no signals in the ^{7}Li NMR window opened up to −20 ppm. It should be mentioned that Li-containing organometallic compounds generally show ^{7}Li NMR signals in the range from 0 to −20 ppm.[19] For example, lithium pentamethylcyclopentadienide (LiCp*) shows a peak at −12.5 ppm,[20] while shifts of ^{7}Li NMR signals up to −16 ppm[10b] are observed for the mixtures of corannulene and substituted fullerenes in the presence of an excess of Li metal. After numerous attempts and variations of experimental conditions, we have successfully crystallized the product from a diglyme/THF solution. The single-crystal X-ray diffraction analysis revealed the formation of an unprecedented mixed-alkali-metal LiK_5 cluster sandwiched between two eclipsed four-fold reduced bowls in $[(C_{20}H_{10}{}^{4-})(LiK_5)^{6+}(C_{20}H_{10}{}^{4-})]^{2-}$ (LiK_5, **1**; Figure 1).

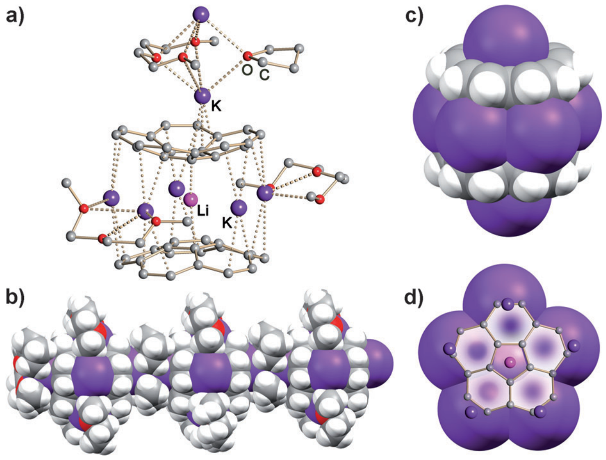

Figure 1. a) Independent unit of **1**; b) 1D crystal packing of the LiK_5 units; c) side view of the space-filling sandwich model; and d) top view of the space-filling drawing superimposed with its ball-and-stick representation.[23]

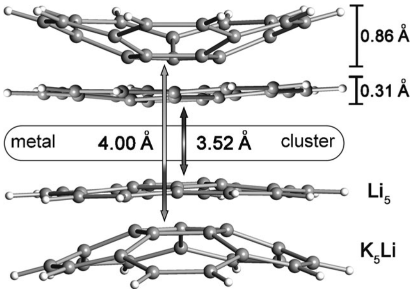

Figure 2. Overlay of the Li_5 and LiK_5 sandwiches (ball-and-stick representation).

All of the Li^+ ions that were encapsulated between the six-membered rings of $C_{20}H_{10}{}^{4-}$ in the Li_5 structure have been replaced by K^+ ions. Satisfyingly, the cavity formed by two central five-membered rings in the triple-decker sandwich is now occupied by a Li^+ ion. As a result, the corannulene surface is fully "saturated" with alkali metals, for the first time reaching the coordination limit for a polyaromatic ligand. In the LiK_5 structure, the distance between the five-membered rings is 4.004(6) Å (Figure 2; Supporting Information, Table S1), which is sufficient to accommodate an additional lithium ion in the inner space. The central Li^+ ion sits right between the two five-membered rings with the Li⋯Cp centroid distance of ca. 2.0 Å. The K⋯C contacts to the six-membered rings of $C_{20}H_{10}{}^{4-}$ range from 2.905(5) to 3.491(5) Å.

The full substitution of lithium ions by potassium ions does not significantly perturb the internal bond length distribution in $C_{20}H_{10}{}^{4-}$ compared to the Li_5 sandwich, but rim C−C bonds in **1** are notably shortened. The latter is a consequence of the substantial curvature increase of corannulene and the subsequent tightening of the rim. The bowl depth of $C_{20}H_{10}{}^{4-}$ reaches an unprecedented high value of 0.860(6) Å, which is about three times greater than that in the Li-only triple-decker supramolecular aggregates (0.241(2)–0.355(2) Å, and comparable to neutral corannulene (0.875(2) Å).[21] It was previously shown for $[Li_5(C_{20}H_{10}{}^{4-})_2]^{3-}$ structures that the bowl depth varies by about 0.3 ± 0.1 Å for three aggregates having different external environments.[11,18a] The direct comparison of the Li_5 with LiK_5 sandwiches

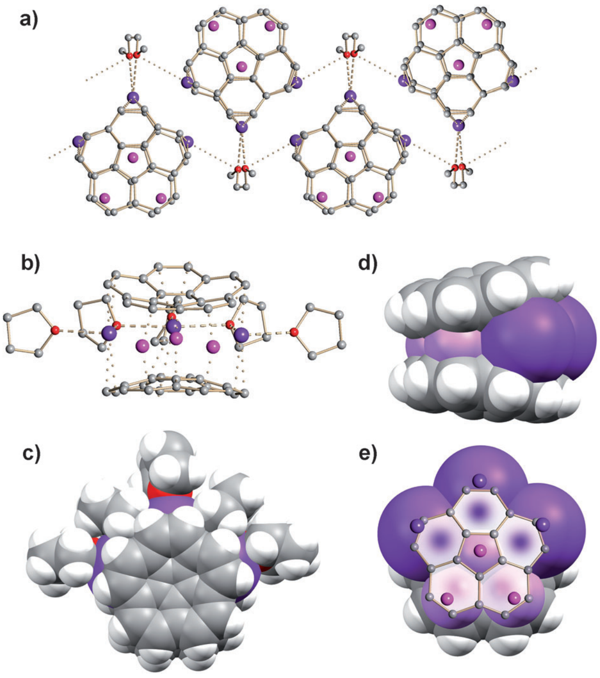

Figure 3. X-ray crystal structures of **2a** ([Li(DME)(12-crown-4)]$_2$-[($C_{20}H_{10}^{4-}$)(Li_3K_3)$^{6+}$($C_{20}H_{10}^{4-}$)(DME)]) and **2b** ([Li(THF)(12-crown-4)]$_2$[($C_{20}H_{10}^{4-}$)(Li_3K_3)$^{6+}$($C_{20}H_{10}^{4-}$)(THF)$_5$]) with the Li_3K_3 metal cluster core. a) Zigzag 1D polymeric chain in **2a**, also showing the eclipsed conformation of corannulene decks; b) ball-and-stick representation of the molecular structure of the Li_3K_3 sandwich in **2b**; c) top and d) side views of the space-filling model of the Li_3K_3 sandwich in **2b**; and e) top view of the space-filling drawing of the sandwich superimposed with its ball-and-stick representation. External Li^+ ions are omitted for both **2a** and **2b**.[23]

illustrates that the difference in the internal composition of the triple-decker sandwiches plays a major effect on the bowl-shaped core. The significant curvature increase of $C_{20}H_{10}^{4-}$ observed in **1** can be explained by the synergism of pushing effects of five large K^+ ions located around the perimeter and pulling effect of the Li^+ ion squeezed in between the central hub rings of corannulene. It illustrates remarkable flexibility of the four-fold reduced corannulene bowls in adapting to different coordination environments, making it an exceptionally versatile π-ligand. In the solid state, two additional K^+ ions occupy the concave bowl cavities at the outside of the LiK_5 sandwich with K···C contacts spanning from 2.803(4) to 3.325(5) Å. Interactions of these ions with bridging diglyme and THF molecules result in the formation of a string-like 1D polymeric chain in the solid state (Figure 1 b).

After we crystallographically confirmed the presence of the hub-bound lithium ion in the LiK_5-sandwich, the ^{7}Li NMR spectra were re-measured using an extended window. Gratifyingly, a single peak appears at the previously concealed high negative value of −22.4 ppm (Supporting Information, Figure S2). This previously unseen record low-field shift shows a need to reconsider the width of a ^{7}Li NMR window for investigation of Li-containing organometallic compounds. This observation is especially important for studies of lithium-doped extended carbon-based materials, such as graphite or graphene, for their use in lithium-ion batteries. Consistent with a very symmetric structure of the LiK_5-aggregate, the ^{1}H NMR spectrum exhibits a single peak at 6.6 ppm (Supporting Information, Figure S1).

Re-investigation by ^{7}Li NMR of the reaction of $C_{20}H_{10}$ monitored in situ with an excess of Li and K in [D$_8$]THF revealed the formation of LiK_5 cluster (−22.4 ppm) along with the broad signal shifted even more to the right end of the spectrum (ca. −24.4 ppm). This implied the existence of another mixed-metal sandwich having greater lithium content than that in **1**. As crystal growth from THF was problematic owing to poor product solubility and formation of undesirable oils, we turned to 1,2-dimethoxyethane (DME) as a potential solvent. We have previously seen that Li-induced reduction of corannulene in DME is accompanied by side-reactions, affording lithium alkoxo-clusters.[22] To avoid these complications, the reaction time should be minimized. However, even with the short reaction times, the in situ ^{7}Li NMR measurements for the mixed Li/K systems in DME showed a variety of peaks owing to the above intrinsic problems. Importantly, a broad new peak appeared where a centrally coordinated lithium cation could be expected. This peak indicated the formation of a new sandwich-type product, which was successfully crystallized by layering the reaction mixture in DME with 12-crown-4 ether in hexanes.

The single-crystal X-ray diffraction analysis revealed a unique supramolecular structure having the Li_3K_3 cluster core squeezed between two four-fold reduced corannulene decks, [($C_{20}H_{10}^{4-}$)(Li_3K_3)$^{6+}$($C_{20}H_{10}^{4-}$)]$^{2-}$ (Li_3K_3, **2a**, Figure 3 a) crystallized along with two [Li(DME)(12-crown-4)]$^+$ cations. The separation between the two bowls in **2a** is slightly smaller than in the LiK_5 sandwich (3.826(5) vs. 4.008(6) Å). Again, all of the coordination sites of $C_{20}H_{10}^{4-}$ are engaged in alkali-metal-ion binding, with one Li^+ ion occupying the central hub ring. In contrast to **1**, two interior Li^+ ions are bound to the neighboring six-membered rings of $C_{20}H_{10}^{4-}$ forming a Li_3 triangle within the Li_3K_3 cluster. In the solid state, the Li_3K_3 sandwiches form a zigzag 1D chain through the K···O interactions with a coordinated DME molecule (3.079(7) Å, Figure 3 a). Notably, the latter chelates one and simultaneously coordinates two other K^+ ions of the neighboring aggregates, thus exhibiting a chelating doubly bridging mode.

The ^{7}Li NMR investigation of Li_3K_3 crystals dissolved in DME revealed that the supramolecular aggregate is stable (single peak at −23.94 ppm) without any signs of product decomposition or metal ion redistribution (Supporting Information, Figure S5). Moreover, the remarkable stability is demonstrated by recrystallization of these crystals from THF. Although all of the coordinated DME molecules in both cationic and anionic parts are replaced by THF, a structure with an essentially unchanged Li_3K_3 core is produced (**2b**; Figure 3 b,c).

Importantly, the triple-decker [($C_{20}H_{10}^{4-}$)(Li_3K_3)$^{6+}$-($C_{20}H_{10}^{4-}$)]$^{2-}$ aggregates crystallize as separate molecular moieties (along with two [Li(THF)(12-crown-4)]$^+$ cations), in contrast to an extended 1D structure of **2a**. This fact denotes that the formation of Li/K sandwiches is not induced by crystal packing, and the specific mixed-metal core can exist in different coordination environments. The separation between the two bowls in **2b** is close to that in **2a** (3.865(2) vs. 3.826(5) Å), additionally illustrating the small effect of external moieties on the geometry of the supramolecular aggregates. Overall, two Li_3K_3 products (**2a** and **2b**) show only small variations in their sandwich core (Supporting Information, Table S3).

As expected, the value of the bowl depth in Li_3K_3 falls almost exactly in between the Li_5 and LiK_5 sandwiches (0.620(2) Å; Supporting Information, Table S1). It was previously shown by ab initio and DFT calculations that the bowl becomes shallower as more electrons are added to its core.[7] Herein, we illustrate for the first time that interactions with encapsulated alkali-metal clusters of different compositions result in a remarkable variation in the bowl depth of $C_{20}H_{10}{}^{4-}$, ranging from 0.24 in Li_5 to 0.62 or even to 0.86 Å in Li_3K_3 and LiK_5 structures, respectively. Such an exceptional curvature manipulation on the molecular level in charged hydrocarbons has not been seen before and can possibly be utilized for storage/release of strain energy.

^1H NMR spectra of Li_3K_3 aggregates are much more complex compared with **1**. In both **2a** and **2b**, two signals for aromatic protons (a sharp signal at 6.8 ppm and a very broad signal at about 6.6 ppm) that do not coalesce upon cooling are observed (Supporting Information, Figures S4,S8). Such behavior is believed to be related to complex dynamic exchange processes involving different parts of the asymmetric Li_3K_3 aggregates in solution. As the proton signal from the homometallic Li_5 sandwich (6.9 ppm, THF) is shifted downfield in comparison with the LiK_5 aggregate (6.6 ppm) having only K^+ ions on the periphery, the broad peak at 6.6 ppm for **2** can be assigned to the protons of $C_{20}H_{10}{}^{4-}$ that are close to the K-enriched part of the Li_3K_3 product. As shown below, the alkali-metal ions are capable of moving in/out through this side only and this affects the associated corannulene protons. Plus, both **2a** and **2b** (grown from DME and THF, respectively) have solvent molecules coordinated to the sandwiched K^+ ions. The scrambling of solvent molecules at these potassium sites on the periphery of Li_3K_3 sandwich can additionally affect the corresponding protons of corannulene causing the observed signal broadening at room temperature. Both processes should slow down at low temperatures resulting in some signal sharpening (Supporting Information, Figure S4). In contrast, two peripheral encapsulated Li^+ ions in **2** are fully shielded by corannulene decks, have no coordinated solvent, and do not provide the path for internal insertion at the Li side of the Li_3K_3 aggregate (as discussed below). The related protons show up as a sharp signal at 6.8 ppm at room temperature. Owing to their nonequivalence, the above signal starts to split at lower temperatures (Supporting Information, Figure S8).

To get further insights into the formation of the unique mixed-alkali-metal supramolecular aggregates discovered in this work, the DFT calculations were performed at the PBE0/def2-TZVPP(Li,K)//cc-pVDZ(C,O,H) level of theory (see the Supporting Information for details). The calculated ^7Li NMR signals for the central Li^+ ion in the Li_3K_3 and LiK_5 organometallic complexes are −26.1 and −23.9 ppm, compared with the experimental values of −23.9 and −22.4 ppm, respectively. Thus, the highly negative values along with the overall dependence on Li/K ratio are reproduced by theory. For the next step, calculations of the whole series of mixed Li/K sandwiches with variable core compositions were carried out (Supporting Information, Table S4). This allows us to discuss the step-by-step changes occurring upon metal exchange starting from the Li-only cluster sandwiched between two $C_{20}H_{10}{}^{4-}$ ligands. The initial formation of a Li_5 sandwich is warranted by the fact that the addition of excess Li metal quickly produces the four-fold reduced anions,[11,18a] while the use of pure K metal affords less charged corannulene species.[6a,c] Starting from the Li_5 cluster, the substitution of small Li^+ ions by larger K^+ ions along the periphery gradually leads to the sandwich opening, simulating the opening of a clamshell (Figure 4, see Li_4K).

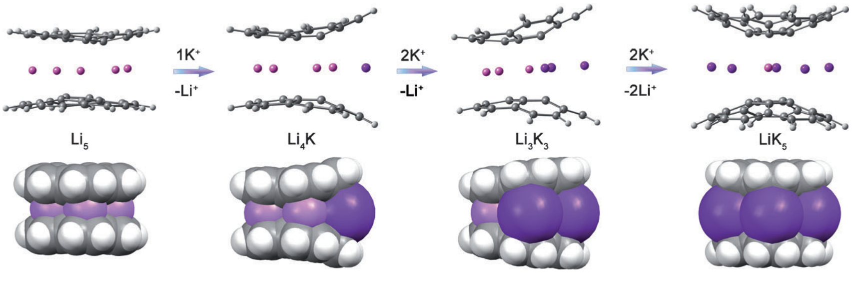

Figure 4. Transformation of alkali-metal cores starting from Li_5 to LiK_5 sandwiches. Some intermediates are omitted.

Herein, the clamshell opening is quantified by measuring angles between the mean planes passing through the rim or hub carbon atoms of $C_{20}H_{10}{}^{4-}$ within the sandwich (Supporting Information, Table S4). The first substitution step in the Li_5 structure leads to a substantial increase of the rim angle (12.8°) in Li_4K, while the five-membered rings of corannulene remain essentially parallel, with the hub angle being unchanged. As a result, the space between the five-membered rings in Li_4K sandwich (3.47 Å) remains small. Thus, substitution of the Li_5 cluster with one K^+ ion does not provide sufficient room between the corannulene decks for incorporation of an additional Li^+ ion in the central position. The second substitution step can afford two isomers, where two K^+ ions are located at either neighboring (α-Li_3K_2) or separated (β-Li_3K_2) benzene rings (Supporting Information, Scheme S1). The substantial increase in both rim and hub angles is observed for this substitution step (Supporting Information, Table S4). Outstandingly, the β-Li_3K_2 isomer, having one Li^+ located between two K^+ ions, shows a substantially lower thermodynamic stability (by ca. 13 kcal mol^{-1}) than the structure with the Li^+ ion being inserted into the space between the five-membered rings of two $C_{20}H_{10}{}^{4-}$ bowls. This provides a considerable driving force for the insertion process with the subsequent formation of the new type of sandwich. Thus, having two K^+ ions separated by one six-membered ring and two Li^+ cations functioning as clamshell hinges on the opposite side open a clamshell sufficiently wide to provide a channel for the interior insertion of a Li^+ ion. This hub-to-ring lithium insertion is essentially barrierless (activation energy, E_a, is calculated to be 0.7 kcal mol^{-1}), and this process is accompanied by a remarkable driving force of about 13 kcal mol^{-1}. The barrier for the reverse process (migration of the central lithium ion back to the rim in between two six-membered rings) is quite significant (13.9 kcal mol^{-1}, Figure 5) with no thermodynamic driving force. After the above insertion is completed, closing the channel with a potassium ion leads to the formation of the stable experimentally observed Li_3K_3 sandwich. The central Li^+ is now fully confined by surrounding alkali metals and has no path to escape.

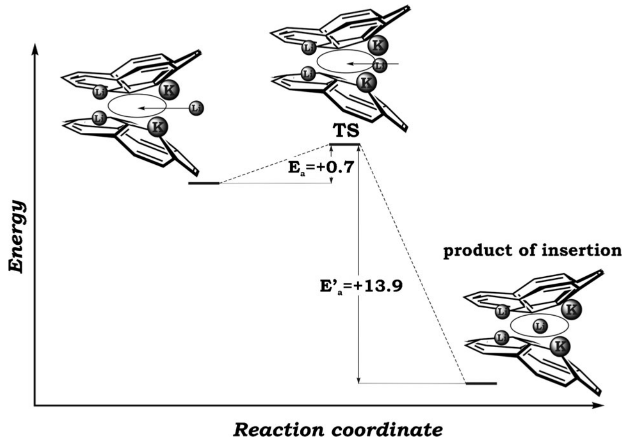

Figure 5. Representation of the Li insertion into the space between two five-membered ring sites.

For comparison, the Li^+ insertion barrier for α-Li_3K_2, where Li could not move in between two K^+ ions, is larger (14.5 kcal mol^{-1}) than in the β-Li_3K_2 sandwich, while the driving force for this process is much lower (2.4 kcal mol^{-1}). The next possible member of the class, Li_2K_4, is readily amenable toward further transformations. The presence of four K^+ ions opens up a clamshell too wide. This makes the last Li^+ ion located between six-membered rings being very weakly bound and easily replaceable by a larger K^+ ion, which fits the allocated space much better. This transformation eventually leads to the formation of the experimentally observed LiK_5 composition.

As a result of these first studies on concomitant alkali metals reduction of a bowl-shaped polyarene, $C_{20}H_{10}$, a new class of mixed-alkali-metal organometallic sandwich compounds has been discovered. Furthermore, the coordination record for the four-fold reduced corannulene, which is able to bind six alkali-metal ions by engaging its five benzene rings along with the central five-membered ring, has been revealed. Notably, the sandwiching of Li^+ ion between the hub sites of two $C_{20}H_{10}{}^{4-}$ bowls is accompanied by unprecedented shifts in ^7Li NMR spectra. This experimental result, augmented by theoretical calculations, illustrates the need to reconsider the width of NMR window for ^7Li NMR investigations of Li-doped extended carbonaceous materials. This work also offers a new approach towards the formation of unique mixed-alkali-metal clusters stabilized by supercharged curved polyarenes. The proposed mechanism of their formation should facilitate the design of other members of this remarkable family and stimulate future practical applications of heavy alkali-metal-doped carbon-based materials.

Received: September 14, 2013

Keywords: alkali metals · curved carbanions · mixed-metal systems · reduced corannulenes · X-ray diffraction

[1] a) X.-D. Xiang, J. G. Hou, V. H. Crespi, A. Zettl, M. L. Cohen, *Nature* **1993**, *361*, 54–56; b) M. J. Rosseinsky, *Chem. Mater.* **1998**, *10*, 2665–2685; c) D. Varshney, N. Singh, *J. Theor. Appl. Phys.* **2012**, *6*, 37–46.

[2] a) R. E. Gerald, R. J. Klingler, G. Sandi, C. S. Johnson, L. G. Scanlon, J. W. Rathke, *J. Power Sources* **2000**, *89*, 237–243; b) S. W. Lee, N. Yabuuchi, G. Naoaki, B. M. Gallant, S. Chen, K. Shuo, H. Byeong-Su, P. T. Hammond, S.-H. Yang, *Nat. Nanotechnol.* **2010**, *5*, 531–537; c) H. Lee, J.-K. Yoo, J.-H. Park, J. H. Kim, K. Kang, Y. Jung, S. Yeon, *Adv. Energy Mater.* **2012**, *2*, 976–982.

[3] H. W. Kroto, J. R. Heath, S. C. O'Brien, F. R. Curl, R. E. Smalley, *Nature* **1985**, *318*, 162–163.

[4] Q. Xie, E. Pérez-Cordero, L. Echegoyen, *J. Am. Chem. Soc.* **1992**, *114*, 3978–3980.

[5] a) K. Prassides, C. Christides, I. M. Thomas, J. Mizuki, K. Tanigaki, I. Hirosawa, T. W. Ebbesen, *Science* **1994**, *263*, 950–954; b) M. B. Boeddinghaus, M. Salzinger, T. F. Fässler, *Chem. Eur. J.* **2009**, *15*, 3261–3267; c) S. Hoffmann, D. Kasinathan, T. F. Fässler, *Inorg. Chem.* **2010**, *49*, 2577–2579; d) K. Y. Amsharov, Y. Krämer, M. Jansen, *Angew. Chem.* **2011**, *123*, 11844–11847; *Angew. Chem. Int. Ed.* **2011**, *50*, 11640–11643; e) N. V. Kozhemyakina, K. Y. Amsharov, J. Nuss, M. Jansen, *Chem. Eur. J.* **2011**, *17*, 1798–1805; f) M. B. Boeddinghaus, B. Wahl, T. F. Fässler, P. Jakes, R.-A. Eichel, *Z. Anorg. Allg. Chem.* **2012**, *638*, 2205–2212.

[6] a) M. Baumgarten, J. L. Gherghel, M. Wagner, A. Weitz, M. Rabinovitz, P.-C. Cheng, L. T. Scott, *J. Am. Chem. Soc.* **1995**, *117*, 6254–6257; b) S. N. Spisak, A. V. Zabula, A. S. Filatov, A. Y. Rogachev, M. A. Petrukhina, *Angew. Chem.* **2011**, *123*, 8240–8244; *Angew. Chem. Int. Ed.* **2011**, *50*, 8090–8094; c) A. V. Zabula, S. N. Spisak, A. S. Filatov, V. M. Grigoryants, M. A. Petrukhina, *Chem. Eur. J.* **2012**, *18*, 6476–6484; d) D. Eisenberg, R. Shenhar, *WIREs Comput. Mol. Sci.* **2012**, *2*, 525–547.

[7] C. Bruno, R. Benassi, A. Passalacqua, F. Paolucci, C. Fontanesi, M. Marcaccio, E. A. Jackson, L. T. Scott, *J. Phys. Chem. B* **2009**, *113*, 1954–1962.

[8] A. Ayalon, M. Rabinovitz, P.-C. Cheng, L. T. Scott, *Angew. Chem.* **1992**, *104*, 1691–1692; *Angew. Chem. Int. Ed. Engl.* **1992**, *31*, 1636–1637.

[9] A. Ayalon, A. Sygula, P.-C. Cheng, M. Rabinovitz, P. W. Rabideau, L. T. Scott, *Science* **1994**, *265*, 1065–1067.

[10] a) T. Sternfeld, R. E. Hoffman, I. Aprahamian, M. Rabinovitz, *Angew. Chem.* **2001**, *113*, 469–471; *Angew. Chem. Int. Ed.* **2001**, *40*, 455–457; b) I. Aprahamian, D. Eisenberg, R. E. Hoffman, T. Sternfeld, Y. Matsuo, E. A. Jackson, E. Nakamura, L. T. Scott, T. Sheradsky, M. Rabinovitz, *J. Am. Chem. Soc.* **2005**, *127*, 9581–9587; c) N. Treitel, T. Sheradsky, L. Peng, L. T. Scott, *Angew. Chem.* **2006**, *118*, 3351–3355; *Angew. Chem. Int. Ed.* **2006**, *45*, 3273–3277.

[11] A. V. Zabula, A. S. Filatov, S. N. Spisak, A. Y. Rogachev, M. A. Petrukhina, *Science* **2011**, *333*, 1008–1011.

[12] a) M. A. Petrukhina, L. T. Scott, *Dalton Trans.* **2005**, 2969 – 2975; b) A. S. Filatov, E. A. Jackson, L. T. Scott, M. A. Petrukhina, *Angew. Chem.* **2009**, *121*, 8625 – 8628; *Angew. Chem. Int. Ed.* **2009**, *48*, 8473 – 8476; c) A. S. Filatov, M. A. Petrukhina, *Coord. Chem. Rev.* **2010**, *254*, 2234 – 2246.

[13] For convenience, all complexes are abbreviated to show the type and the number of metals incorporated between the hydrocarbon decks.

[14] M. S. Dresselhaus, G. Dresselhaus, *Adv. Phys.* **2002**, *51*, 1 – 186.

[15] S. Harder, M. H. Prosenc, *Angew. Chem.* **1994**, *106*, 1830 – 1832; *Angew. Chem. Int. Ed. Engl.* **1994**, *33*, 1744 – 1746.

[16] a) D. Stalke, *Angew. Chem.* **1994**, *106*, 2256 – 2259; *Angew. Chem. Int. Ed. Engl.* **1994**, *33*, 2168 – 2171; b) R. E. Dinnebier, U. Behrens, F. Olbrich, *Organometallics* **1997**, *16*, 3855 – 3858.

[17] a) R. E. Mulvey, *Acc. Chem. Res.* **2009**, *42*, 743 – 755; b) A. R. Kennedy, J. Klett, R. E. Mulvey, D. S. Wright, *Science* **2009**, *326*, 706 – 708; c) R. E. Mulvey, V. L. Blair, W. Clegg, A. R. Kennedy, J. Klett, L. Russo, *Nat. Chem.* **2010**, *2*, 588 – 591.

[18] a) A. V. Zabula, S. N. Spisak, A. S. Filatov, M. A. Petrukhina, *Organometallics* **2012**, *31*, 5541 – 5545; b) D. Eisenberg, J. M. Quimby, D. Ho, R. Lavi, L. Benisvy, L. T. Scott, R. Shenhar, *Eur. J. Org. Chem.* **2012**, 6321 – 6327.

[19] R. Michel, R. Herbst-Irmer, D. Stalke, *Organometallics* **2011**, *30*, 4379 – 4386.

[20] B.-Y. Tay, C. Wang, L. P. Stubbs, C. Jacob, M. van Meurs, *J. Organomet. Chem.* **2011**, *696*, 3431 – 3435.

[21] M. A. Petrukhina, K. W. Andreini, J. Mack, L. T. Scott, *J. Org. Chem.* **2005**, *70*, 5713 – 5716.

[22] A. V. Zabula, S. N. Spisak, A. S. Filatov, M. A. Petrukhina, *Angew. Chem.* **2012**, *124*, 12360 – 12364; *Angew. Chem. Int. Ed.* **2012**, *51*, 12194 – 12198.

[23] CCDC 934964 (**2a**), CCDC 934965 (**2b**), and CCDC 934966 (**1**) contain the supplementary crystallographic data for this paper. These data can be obtained free of charge from The Cambridge Crystallographic Data Centre via www.ccdc.cam.ac.uk/data_request/cif.